BASELINE CHARACTERIZATION OF MOISTURE ADSORPTION AND THERMAL VARIATION IN LHS-1E FOR LUNAR ROVER OPERATIONS. A. S. Glover[1], B. D. Byron[2], P. Tripathi[2], M. P. Lucas[3], J. M. Long-Fox[2], C. R. Neal[4], J. Brisset[3], D. Britt[2], and K. L. Donaldson Hanna[2], [1]University of Central Florida's (UCF) Exolith Lab ®, 532 S. Econ Cir STE 100, Oviedo, FL 32765, (abigail.glover@ucf.edu), [2]UCF Department of Physics, 4111 Libra Dr, Orlando, FL 32816, [3]Florida Space Institute, UCF, Partnership I, Research Pkwy, Orlando, FL 32826, [4]University of Notre Dame Department of Civil & Environmental Engineering & Earth Sciences, Notre Dame, IN 46556

Introduction: Understanding the geotechnical properties of lunar regolith simulants and how they vary is essential for future rover operations and *in situ* resource utilization (ISRU) to support long-term lunar infrastructure [1]. Moisture adsorption and thermal behavior in simulants significantly impacts factors such as compaction, wheel interactions, and regolith processing for resource extraction [2]. In this study, we establish baseline measurements of moisture content and thermal variation in Space Resource Technologies (SRT) Engineering Grade Lunar Highlands Simulant (LHS-1E) using the Regolith Interactions for the Development of Extraterrestrial Rovers (RIDER) testbed at the University of Central Florida (UCF) [3].

Methods: Regolith Interactions for the Development of Extraterrestrial Rovers (RIDER) is a large-scale (3.8 m long × 0.9 m wide × 0.5 m deep) terramechanics testbed located at UCF's Exolith Lab [4]. The facility offers novel capabilities for examining regolith terramechanics and rover wheel interactions with the ability to support lunar and martian terrains (Fig. 1). RIDER can simulate a variety of rover masses and accepts a wide range of wheel sizes while allowing adjustments for motor speed and torque through interchangeable motors [4].

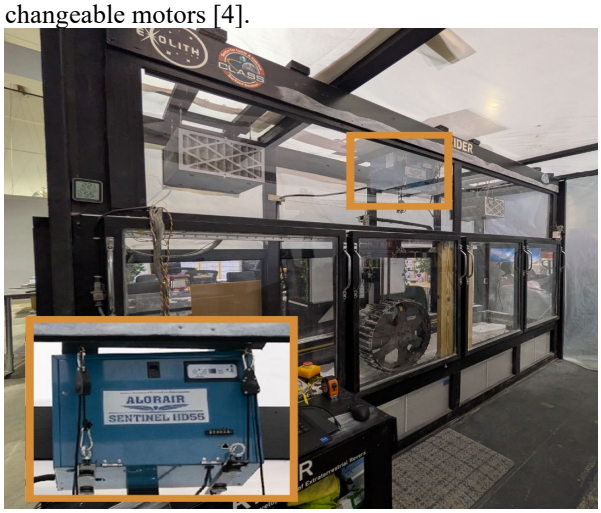

Figure 1: RIDER facility at UCF's Exolith Lab, with dehumidifier unit outlined in orange.

Moisture Content This study utilized pre-existing environmental control systems in the RIDER testbed. Specifically, an Alorair HD55 industrial dehumidifier (Fig. 1) dried the internal chamber of the RIDER testbed for a minimum of 8 hours (maximum 48 hours) before sample collection. Simulant was examined in two configurations: (1) the testbed was filled with a single layer of LHS-1E to a depth of 30 cm and compacted to a density of ~1.75 g/cm^3, and (2) ~ 2-3 cm of loose simulant was added on the surface layer of the compacted simulant. Surface and core samples were taken at three locations along the length of the testbed under humidity-adjusted conditions to examine moisture content utilizing ASTM D2216-19 [5]. Temperature and relative humidity were recorded using two thermo-hygrometers located on each end of the bin, and one in the upper chamber. A simplified airflow model of the RIDER testbed was created using SolidWorks to analyze airflow patterns resulting from running the dehumidifier for comparison.

Surface Thermal Variation The RIDER testbed was filled to a depth of 30 cm with LHS-1E in a single layer at ~1.58 g/cm^3 density, then an Astrobotic Polaris prototype wheel was rolled over the surface at an average speed of 9 cm/s and with varying loads (5 – 50 kg) to simulate potential wheel conditions at lunar gravity. Temperature and image data were collected after every 10 wheel passes for a total of 100 passes (50 in each direction). Temperatures were measured from 3 locations directly underneath an infrared heating device for comparison: (1) the broad, flat part of the track, (2) the indented part created by grousers, and (3) the nearby undisturbed simulant outside the track. Locations 1, 2, and 3 were evaluated, selected, and documented after every set of 10 wheel passes to maintain the initial x-y coordinates in the testbed while upholding relative depth comparisons.

An initial thermal infrared (TIR) image of the heating site was taken before interacting with the rover wheel. Baseline data was collected by heating the undisturbed simulant using a 500W infrared heater 14.6 cm above the surface. TIR images (FLIR Boson camera) and temperature readings (laser thermometer with an accuracy of ± 2°C and emissivity of 0.95; [6, 7, 8]) of the simulant were collected every 150 seconds until readings were within ± 1°C of the previous, indicating equilibrium had been reached. When a maximum tem-

perature was observed, the heater was removed and data collection continued through the cooling process until readings were within ± 1°C of each other.

Results and Discussion:

Moisture Content Water in lunar regolith is primarily concentrated on the outer surface of regolith grains, making its distribution highly dependent on the surface-to-volume ratio [9]. The specific surface area (SSA) of the regolith simulant used in this study (0.474 m^2/g, [10]) is comparable to lunar highlands regolith [11], allowing for meaningful comparisons. Data from the Chang'E-5 lander estimated up to 120 ppm of water (OH + H_2O) in the lunar regolith, attributing this moisture to surface-layer adsorption and subsurface retention [9].

In this study, simulant moisture content across the RIDER testbed exhibited significant spatial variation. The left side displayed unexpected increases in moisture at lower relative humidities, while the center maintained a steadier trend. The right side, which showed the lowest average relative humidity, aligned well with simulation results (Fig. 2, 3). However, core samples, largely unaffected by surface-level humidity fluctuations, exhibited consistent moisture content, suggesting that initial compaction conditions played a significant role in moisture retention. The moisture content measurements varied by as much as 72% beyond the Chang'E-5 estimates, suggesting extreme variability even after exposure to controlled environmental conditions such as dehumidification [9].

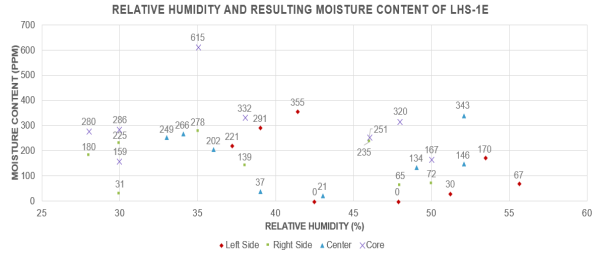

Figure 2: Key data comparing moisture content at various relative humidity levels within RIDER.

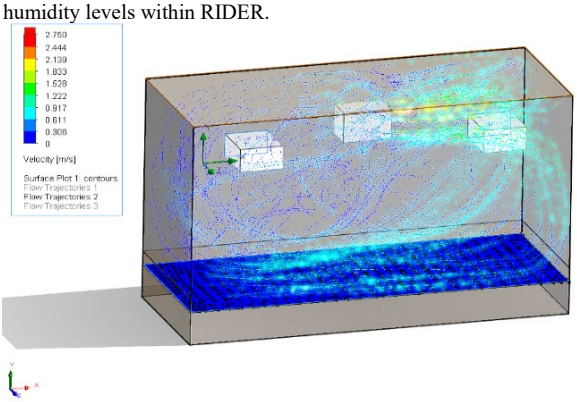

Figure 3: Fluid flow simulation within RIDER.

Thermal Variation The captured images show distinct surface temperatures for the different regions of the wheel track during the heating and cooling process (Fig. 4). For instance, some of the wheel track grouser locations that are pointed away from the heat source were cooler during the warming phase due to not receiving direct irradiance from the heat source (Fig. 4B). However, after significant exposure to thoroughly heated surrounding simulant, the temperatures at these locations become relatively warmer than those at the surface due to heat conducting downward throughout the simulant (Fig. 4C). When comparing the undisturbed simulant with simulant that had interacted with the wheel, some regions in the tracks created by the wheel grousers retained comparatively less heat whereas other regions were about the same.

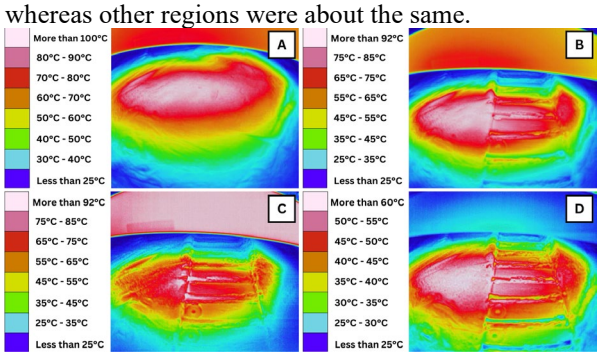

Figure 4: (A) Thermal image of undisturbed LHS-1E, **(B)** Thermal image of rover path after initial heating, **(C)** Thermal image of rover path after maximum heating, **(D)** Thermal image of rover path during cool down.

Conclusion: This research investigated moisture content levels and temperature variations in LHS-1E due to rover wheel interaction to establish a baseline relationship under terrestrial conditions, enabling more informed rover operation and wheel testing strategies. This work contributes to a deeper understanding of regolith simulant geotechnical properties for informed preparation of long-term infrastructure, development, and resource utilization.

References: [1] Dotson et al. (2024) *55th LPSC* Abstract #1726. [2] Long-Fox et al. (2022) *ASCE Earth & Space.* [3] Space Resource Technologies. (Dec. 2022) *LHS-1E Spec Sheet.* [4] Long-Fox et al. (2024) *LSIC Spring Meeting*. [5] ASTM Standard D2216-19 (2019) [6] Tripathi et al. (2023) *Acta Astro, 204,* 263-280. [7] McCloy et al. (2011) *Review Sci. Inst., 82.5,* doi: 10.1063/1.3590016. [8] Matyas et al. (2009) *Pacific Northwest National Lab (PNNL*), No. PNNL-18872. Lin et al. (2024) *Science Bulletin,* pgs. 3723-3729. [9] Lin et al. (2022) *Sci. Adv.,* Volume 8 Issue 1. [10] Long-Fox et al. (2022) *53rd LPSC* Abstract #1594. [11] Kring et al. (2006) *Lunar Exploration Initiative.*